Constitutive dynein activity in *she1* mutants reveals differences in microtubule attachment at the yeast spindle pole body

Zane J. Bergman*, Xue Xia, I. Alexandra Amaro[†], and Tim C. Huffaker
Department of Molecular Biology and Genetics, Cornell University, Ithaca, NY 14853

ABSTRACT The organization of microtubules is determined in most cells by a microtubule-organizing center, which nucleates microtubule assembly and anchors their minus ends. In *Saccharomyces cerevisiae* cells lacking She1, cytoplasmic microtubules detach from the spindle pole body at high rates. Increased rates of detachment depend on dynein activity, supporting previous evidence that She1 inhibits dynein. Detachment rates are higher in G1 than in metaphase cells, and we show that this is primarily due to differences in the strengths of microtubule attachment to the spindle pole body during these stages of the cell cycle. The minus ends of detached microtubules are stabilized by the presence of γ-tubulin and Spc72, a protein that tethers the γ-tubulin complex to the spindle pole body. A Spc72–Kar1 fusion protein suppresses detachment in G1 cells, indicating that the interaction between these two proteins is critical to microtubule anchoring. Overexpression of She1 inhibits the loading of dynactin components, but not dynein, onto microtubule plus ends. In addition, She1 binds directly to microtubules in vitro, so it may compete with dynactin for access to microtubules. Overall, these results indicate that inhibition of dynein activity by She1 is important to prevent excessive detachment of cytoplasmic microtubules, particularly in G1 cells.

INTRODUCTION

Proper function of microtubules depends on their correct organization within cells. In most cells, microtubules are organized by the microtubule-organizing center (MTOC), which nucleates microtubule assembly. Microtubule plus ends extend outward from the MTOC, creating a polarized array of microtubules that the cell uses for the directional transport of vesicles, organelles, and chromosomes (reviewed in Desai and Mitchison, 1997). Because many of these transport events involve the movement of large cargoes, they must generate considerable force. For example, in yeast, single microtubules are used to pull the nucleus toward the bud neck and

chromosomes toward the spindle poles (O'Toole *et al.*, 1999). Thus the anchoring of microtubules to the MTOC must be strong enough to withstand these forces.

The MTOC in the budding yeast, *Saccharomyces cerevisiae*, is the spindle pole body (SPB), an ~0.5-GDa structure that is embedded in the nuclear membrane (reviewed in Jaspersen and Winey, 2004). The SPB is a trilaminar, disk-shaped structure: a central plaque spans the nuclear envelope, an outer plaque faces the cytoplasm, and an inner plaque faces the nucleoplasm. Early in the cell cycle, a structure termed the half-bridge is adjacent to one side of the central plaque. Subsequent SPB duplication produces side-by-side SPBs that are separated by a bridge that is twice the size of the half-bridge. SPB separation severs the bridge, and SPBs with their associated half-bridges move to opposite sides of the nuclear envelope to form the spindle poles.

The γ-tubulin complex nucleates microtubules at the SPB (Marschall *et al.*, 1996; Spang *et al.*, 1996). In yeast, the γ-tubulin complex contains the γ-tubulin protein Tub4, Spc97, and Spc98 (Knop and Schiebel, 1997). In the cytoplasm, this complex is linked to the SPB through Spc72 (Knop and Schiebel, 1998). In G1 cells, Spc72 is primarily unphosphorylated and binds to Kar1, which is located in the half-bridge. As cells enter S phase and proceed

through mitosis, Spc72 becomes phosphorylated and binds preferentially to Nud1, a component of the outer plaque (Pereira *et al.*, 1999). Therefore, cytoplasmic microtubules primarily arise from the half-bridge during G1 and from the outer plaque during mitosis.

The primary role of cytoplasmic microtubules in yeast is to orient the spindle. Two pathways contribute to spindle orientation. Early in the cell cycle a complex of Bim1, Kar9, and Myo2 associates with the plus end of the cytoplasmic microtubule (Korinek *et al.*, 2000; Lee *et al.*, 2000; Yin *et al.*, 2000). Myo2 is a myosin V protein that translocates along polarized actin cables into the bud, thereby pulling the microtubule and its attached SPB toward the bud neck (Yin *et al.*, 2000; Hwang *et al.*, 2003). This event places the metaphase spindle adjacent to the bud neck. Later in the cell cycle, a second pathway involving dynein ensures that the elongating spindle passes through the bud neck and into the bud (Moore *et al.*, 2009). During anaphase, dynactin is recruited to the cytoplasmic microtubule plus end, where it activates dynein. Dynein then interacts with Num1, a protein bound to the bud cortex. Here the minus end–directed motor activity of dynein reels in the cytoplasmic microtubule, thereby pulling the attached SPB into the bud (Farkasovsky and Küntzel, 1995; Heil-Chapdelaine *et al.*, 2000; Lee *et al.*, 2005; Markus and Lee, 2011).

To ensure the proper timing of dynein function, its activity is restricted to a small portion of the cell cycle around anaphase (reviewed in Moore *et al.*, 2009). Dynein is found on cytoplasmic microtubules during the majority of the cell cycle, so the timing of dynein activity is believed to depend on the loading of the dynactin complex, which becomes enriched at cytoplasmic microtubule plus ends during anaphase (Woodruff *et al.*, 2009). She1 inhibits the loading of the dynactin complex onto microtubule ends at other stages of the cell cycle (Woodruff *et al.*, 2009). In this study, we show that She1 activity is important to prevent high rates of cytoplasmic microtubule detachment from the SPB. We characterize the molecular nature of these detachment events, show that their frequency depends on the way in which cytoplasmic microtubules are anchored to the SPB, and propose a model for She1 action.

RESULTS

Detachment of cytoplasmic microtubules from the SBP in *she1Δ* mutants depends on the cell cycle and dynein activity

We noticed that cytoplasmic microtubules in *she1Δ* cells frequently detached from their anchor point at the SPB and moved freely around the cell periphery before depolymerizing (Figure 1A and Supplemental Video S1). Similar cytoplasmic microtubule detachment from the SPB was previously observed in cells containing *cnm67Δ* or *SPC72^stu2Δ* mutations, which affect the integrity of the SPB outer plaque (Hoepfner *et al.*, 2000; Usui *et al.*, 2003). We quantified this effect by determining the fraction of cytoplasmic microtubules that detach from the SPB per minute. In asynchronously growing wild-type cells only 0.02% of microtubules detach (Figure 1B). In contrast, in asynchronously growing *she1Δ* cells 0.7% of microtubules detach.

Further observation of microtubule detachment in asynchronous cultures revealed that the majority of these events occurred in cells that were growing early in the cell cycle, before the formation of a bipolar spindle. To measure this difference, we created uniform populations of cells by arresting them either in G1, by exposure to α-factor, or in metaphase, by depletion of Cdc20. During G1 arrest, 0.1% of microtubules detach in wild-type cells and 1.5% of microtubules detach in *she1Δ* cells (Figure 1B). During metaphase arrest, 0.02% of microtubules detach in wild-type cells and 0.2% of microtubules detach in *she1Δ* cells. Thus, in wild-type and *she1Δ* cells microtubule detachment is five- and eightfold more frequent,
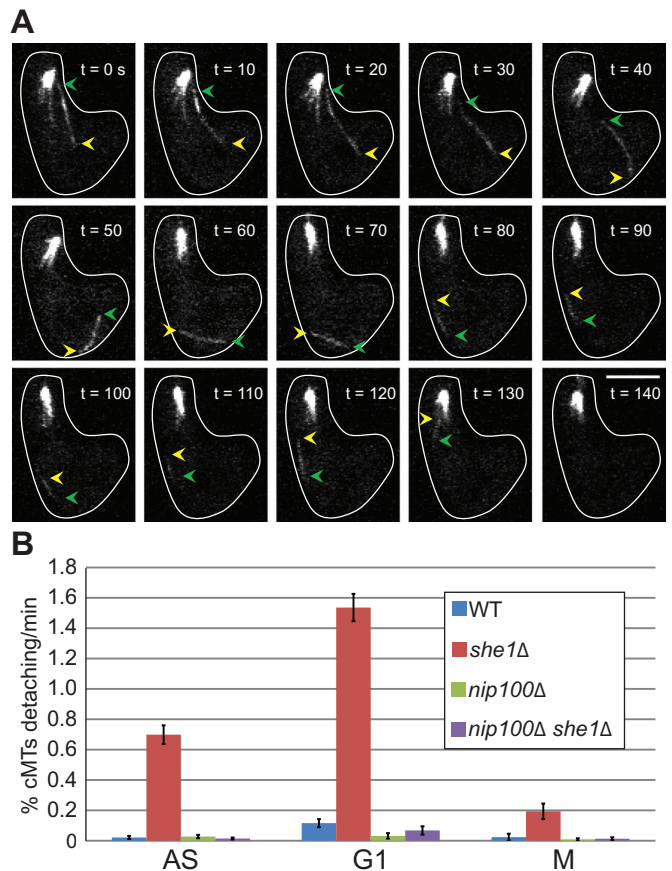

FIGURE 1: *she1Δ* increases the rate of cytoplasmic microtubule detachment from the SPB. (A) Time-lapse images of a G1-arrested *she1Δ* cell expressing GFP-Tub1. The yellow arrowheads point to the plus end and the green arrowheads point to the minus end of a cytoplasmic microtubule that detaches from the SPB. Each frame advances 10 s. Scale bar, 5 µm. See Supplemental Video S1. (B) Rates of cytoplasmic microtubule detachment in wild-type (WT; CUY2015 and CUY2018), *she1Δ* (CUY2016 and CUY2019), *nip100Δ* (CUY1991 and CUY2033), and *nip100Δ she1Δ* (CUY2017 and CUY2034) cells. AS, asynchronous cells; G1, G1-arrested cells; M, metaphase-arrested cells. Data are given in Supplemental Table S1.

respectively, in G1 than in metaphase. In G1 and metaphase cells, microtubule detachment is 15- and 10-fold more frequent, respectively, in *she1Δ* cells than in wild-type cells.

Woodruff *et al.* (2009) reported that She1 limits dynein activity to anaphase by inhibiting the recruitment of dynactin to cytoplasmic microtubule ends at other points in the cell cycle. This result suggests that the increased microtubule detachment observed in *she1Δ* cells is likely due to untimely dynein activity. To test this possibility, we measured microtubule detachment in cells lacking the dynactin complex protein Nip100, which is essential for dynein activity. Microtubule detachment rates in *she1Δ nip100Δ* cells were even less than those in wild-type cells for asynchronous, G1, and metaphase populations (Figure 1B). Thus the increased frequency of microtubule detachment in *she1Δ* cells depends on dynein activity.

Detachment rate depends on the site of cytoplasmic microtubule anchorage

We were curious as to why the microtubule detachment rate differed between G1 and metaphase. In cycling cells, cytoplasmic microtubules originate from both the outer plaque and half-bridge
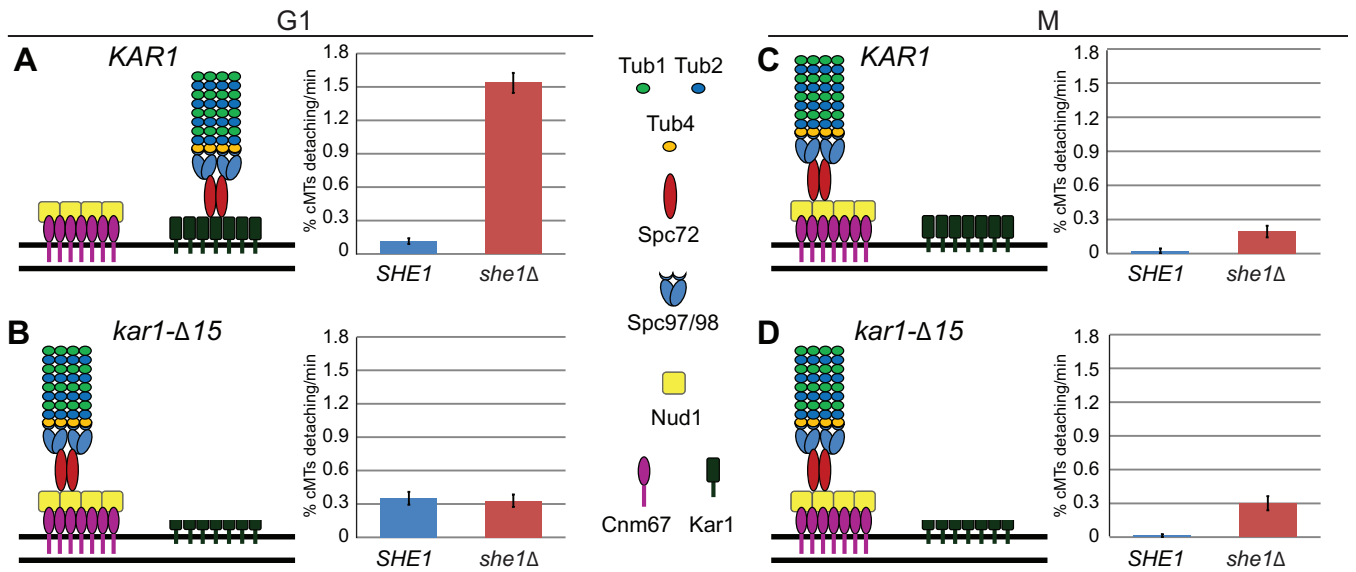
FIGURE 2: (A) In wild-type (*KAR1*) G1 cells, Spc72 binds to Kar1 and microtubules are nucleated from the half-bridge. Graph shows cytoplasmic microtubule detachment rate in *KAR1* (CUY2015) and *KAR1 she1Δ* (CUY2016) G1 cells. (B) The *kar1-Δ15* mutation eliminates the Spc72-binding site on Kar1; therefore, microtubules nucleate from the outer plaque in G1 *kar1-Δ15* cells. Graph shows microtubule detachment rate in *kar1-Δ15* (CUY2008) and *kar1-Δ15 she1Δ* (CUY2009) G1 cells. (C) In wild-type (*KAR1*) metaphase cells, Spc72 binds to Nud1, and microtubules are nucleated from the outer plaque. Graph shows microtubule detachment rate in *KAR1* (CUY2018) and *KAR1 she1Δ* (CUY2019) metaphase cells. (D) The *kar1-Δ15* mutation does not affect the binding of Spc72 to Nud1; therefore, microtubule attachment to the outer plaque at metaphase is not altered. Graph shows cytoplasmic microtubule detachment rate in *kar1-Δ15* (CUY2020) and *kar1-Δ15 she1Δ* (CUY2021) metaphase cells. G1, G1-arrested cells; M, metaphase-arrested cells. Data are given in Supplemental Table S1.

during the early portion of the cell cycle but extend exclusively from the outer plaque once the spindle has formed (Byers and Goetsch, 1975; O'Toole *et al.*, 1999; Pereira *et al.*, 1999). In cells arrested in G1 by treatment with α-factor, cytoplasmic microtubules originate only from the half-bridge (Figure 2A). Hence, cells arrested in G1 by exposure to α-factor and in metaphase by depletion of Cdc20 contain cytoplasmic microtubules that originate only from the half-bridge and outer plaque, respectively. Because cytoplasmic microtubules originate from two alternate locations in G1 and metaphase cells, detachment rates could reflect differences in the strengths of attachment of microtubules to the SPB. An alternative explanation is that the amount of force pulling on cytoplasmic microtubules could differ during G1 and metaphase. To distinguish between these two possibilities, we wanted to compare detachment rates from these two locations in the same cell cycle state. To this end, we created a strain in which cytoplasmic microtubules are nucleated from the outer plaque even when arrested in G1. The *kar1-Δ15* mutation deletes the portion of Kar1 that binds Spc72 and thus eliminates cytoplasmic microtubule nucleation from the half-bridge (Vallen *et al.*, 1992; Pereira *et al.*, 1999). In metaphase cells, when cytoplasmic microtubules normally nucleate from the outer plaque, we predicted that the *kar1-Δ15* mutation should have little effect on cytoplasmic microtubule detachment, and this is what we observed for *SHE1* and *she1Δ* cells (Figure 2, C and D).

In G1 cells, we observed about half the normal number of cytoplasmic microtubules in *kar1-Δ15* and *kar1-Δ15 she1Δ* cells (2.1 microtubules per wild-type cell and 1.0 microtubule per *kar1-Δ15* cell). These cytoplasmic microtubules presumably arise from the outer plaque where Spc72 binds to Nud1. At this stage of the cell cycle, when Spc72 binding to Kar1 is normally favored, binding to Nud1 is not optimal (Pereira *et al.*, 1999). In addition to reduced cytoplasmic

microtubule numbers, we observed a significant number of cytoplasmic microtubules in *kar1-Δ15* and *kar1-Δ15 she1Δ* cells that are not attached to the SPB (0.5 ± 0.1 and 0.6 ± 0.1 per cell, respectively). Although these might have detached from the SPB, it seems more likely they are nucleated by cytoplasmic aggregates of Spc72 that fail to bind to the SPB (Vallen *et al.*, 1992; Pereira *et al.*, 1999). The *kar1-Δ15* mutation also increased the rate of cytoplasmic microtubule detachment threefold above that observed in wild-type cells. Although we do not know the mechanism of this increased rate of release, we refer to it as spontaneous release because it does not depend on dynein activity; introducing the *nip100Δ* mutation does not lower cytoplasmic microtubule detachment in *kar1-Δ15* cells (Supplemental Table S1).

Using the *kar1-Δ15* mutation, we could measure the effect of *she1Δ* on microtubule detachment from both the half-bridge (*she1Δ* cells) and the outer plaque (*kar1-Δ15 she1Δ* cells) at the same point in the cell cycle (G1). In G1 *kar1-Δ15 she1Δ* cells, the cytoplasmic microtubule detachment rate is nearly fourfold lower than in *she1Δ* cells (Figure 2, A and B). This rate is similar to the spontaneous release rate observed in *kar1-Δ15* cells, indicating that *she1Δ* has relatively little effect in *kar1-Δ15* cells. The *nip100Δ* mutation does not lower microtubule detachment in *kar-15Δ she1Δ* cells, indicating that this residual release is not due to dynein activity (Supplemental Table S1). Thus microtubule attachment to the outer plaque, even under suboptimal conditions, is stronger than the normal microtubule attachment to the half-bridge.

Detached microtubules possess γ-tubulin and Spc72

We next set out to establish the place at which cytoplasmic microtubule detachment occurs. The first aim was to find whether cytoplasmic microtubules broke somewhere along the length of
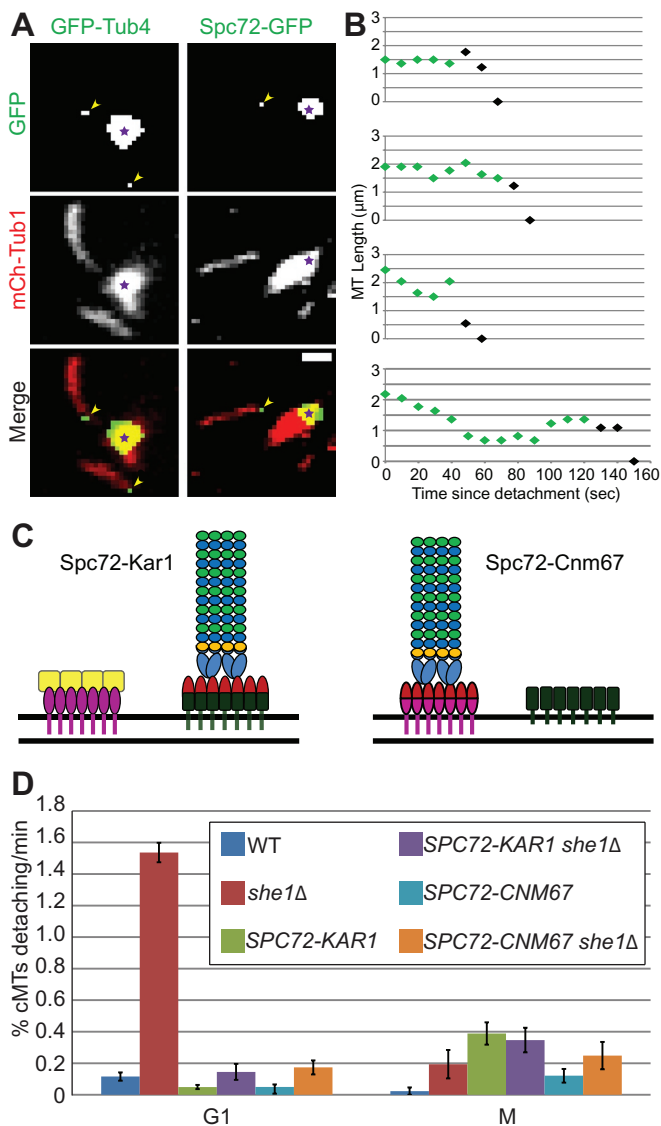
FIGURE 3: Detached cytoplasmic microtubules contain γ-tubulin and Spc72. (A) Detached cytoplasmic microtubules in G1-arrested *she1Δ* cells expressing mCherry-Tub1 and GFP-Tub4 (left, CUY2028) or mCherry-Tub1 and Spc72-GFP (right, CUY2037). Arrowheads indicate GFP signal at the minus ends of detached microtubules. Stars indicate SPBs. Scale bar, 2 μm. (B) Graphs of microtubule lengths after detachment from the SPB. Time 0 is defined as the frame when the microtubule detaches. Green points indicate the presence of GFP-Tub4 at the minus end; black points indicate that the GFP signal is not detected. (C) Diagram shows that cytoplasmic microtubules nucleate from the half-bridge in cells expressing the Spc72–Kar1 fusion protein and from the outer plaque in cells expressing the Spc72-Cnm67 fusion protein in both G1 and metaphase cells. Key to proteins as in Figure 2. (D) Rate of cytoplasmic microtubule detachment in wild-type (WT; CUY2015 and CUY2018), *she1Δ* (CUY2016 and CUY2019), *SPC72-KAR1* (CUY2010 and CUY2025), *SPC72-KAR1 she1Δ* (CUY2011 and CUY2035), *SPC72-CNM67* (CUY2022 and CUY2024), and *SPC72-CNM67 she1Δ* (CUY2023 and CUY2030) cells. G1, G1-arrested cells; M, metaphase-arrested cells. Data are given in Supplemental Table S1.

the polymer or whether they were pulled intact from the SPB. If the latter were true, it might be possible to observe anchoring proteins from the γ-tubulin complex or even the SPB on the minus ends of detached cytoplasmic microtubules. We initially imaged

she1Δ cells in G1 expressing mCherry-Tub1 and green fluorescent protein (GFP)–Tub4 (Figure 3A). Of the 72 cytoplasmic microtubules observed detaching from the SPB, 62 (86%) had visible GFP-Tub4 at the end detaching from the SPB. We also imaged cytoplasmic microtubule detachment in *she1Δ* cells in G1 expressing mCherry-Tub1 and Spc72-GFP (Figure 3A). Spc72-GFP was observed on the ends of 21 of 26 (81%) detached cytoplasmic microtubules. On the other hand, we never observed Spc42 on the ends of detached cytoplasmic microtubules in cells expressing GFP-Tub1 and Spc42-mRFP. This result was expected, since Spc42 is in the central core of the SPB. In summary, these results indicate that detached cytoplasmic microtubules contain γ-tubulin and Spc72 at their minus ends, indicating that the break must occur somewhere on the SPB-proximal side of Spc72.

We also measured the lifetime of 10 detached cytoplasmic microtubules in *she1Δ* cells expressing mCherry-Tub1 and GFP-Tub4; 4 of these are plotted in Figure 3B. The GFP-Tub4 decoration remained on the minus ends of detached microtubules for 69 ± 38 s. During this time some microtubules elongated, some shortened, and some remained fairly constant in length. After loss of the GFP-Tub4 decoration, microtubules inevitably shortened and disappeared in 17 ± 7 s. Thus the minus ends of detached cytoplasmic microtubules appear to be stabilized initially against depolymerization by the presence of a cap of γ-tubulin and associated proteins. Loss of this cap results in rapid depolymerization of the microtubule.

We next examined whether the break point in G1 cells was between Spc72 and Kar1. Spc72[1-276]–Kar1[192-433] is a fusion protein that combines the γ-tubulin complex–binding portion of Spc72 and the half-bridge-binding region of Kar1 (Pereira *et al.*, 1999). This construct was expressed in a strain lacking the native Spc72 and Kar1 proteins, so that the only source of these proteins is the fusion protein (Figure 3C). Thus all cytoplasmic microtubules in these cells are anchored at the half-bridge through the Spc72–Kar1 fusion protein. Addition of the Spc72–Kar1 fusion protein lowers the rates of cytoplasmic microtubule detachment twofold in wild-type cells and 11-fold in *she1Δ* cells (Figure 3D). Because the fusion protein substantially reduces cytoplasmic microtubule detachment, we conclude that the interaction between Spc72 and Kar1 is the linkage that is normally broken during this process in G1 cells.

We used a second fusion protein to examine whether the break point in metaphase cells was between Spc72 and Cnm67. Spc72[1-276]–Cnm67[1-581] is a fusion protein that combines the Tub4-binding region of Spc72 and the outer plaque–binding portion of Cnm67 (Gruneberg *et al.*, 2000). This fusion protein bypasses the need for Nud1 that normally bridges these two proteins. Cells expressing the Spc72–Cnm67 fusion lack the native Spc72, so the only source of cytoplasmic microtubule anchoring is through the fusion protein located in the outer plaque (Figure 3C). The presence of the Spc72–Cnm67 fusion protein did not reduce the rate of cytoplasmic microtubule detachment; in fact detachment rates rose fivefold in wild-type cells and 1.3-fold in *she1Δ* cells (Figure 3D). Thus we cannot conclude that it is the linkage between Spc72 and Cnm67 that is normally broken during cytoplasmic microtubule detachment in metaphase cells.

Of interest, the Spc72–Kar1 fusion did not reduce cytoplasmic microtubule detachment rates in metaphase-arrested cells; in fact these rates rose 17-fold in wild-type and twofold in *she1Δ* cells (Figure 3D). Thus, even the enhanced stability provided by this fusion protein at the half-bridge is still less than that provided by the normal outer plaque connection in metaphase cells. In addition, the Spc72–Cnm67 fusion reduced the rate of cytoplasmic microtubule detachment in G1 cells: twofold for wild-type cells and ninefold
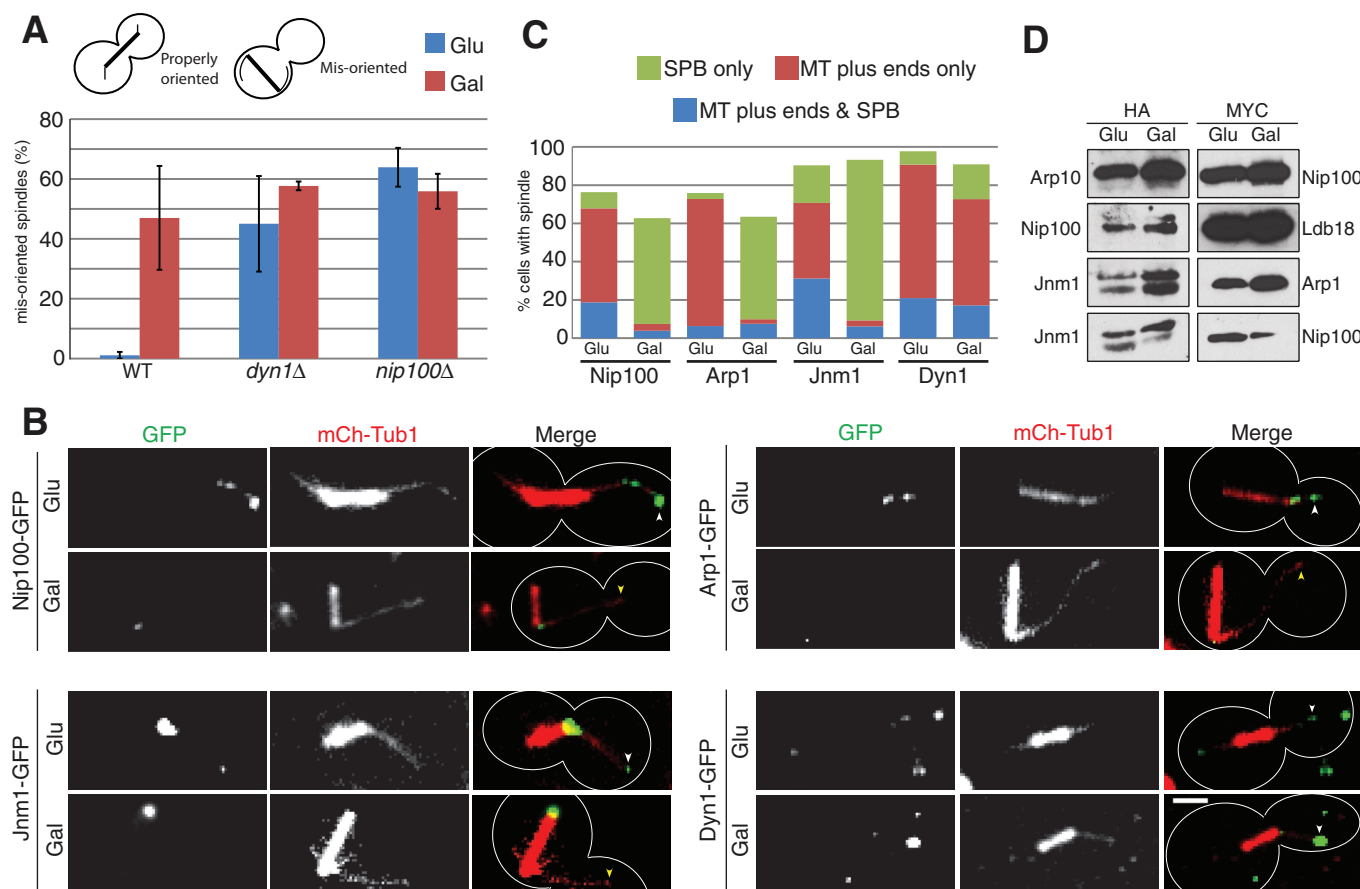
FIGURE 4: Overexpression of She1 inhibits localization but not assembly of the dynactin complex. Cells contained a *SHE1* construct expressed from the *GAL1/10* promoter on a plasmid. *SHE1* was overexpressed by shifting cells to galactose-containing medium for 4 h. (A) Quantification of spindle misorientation. Midanaphase spindles (3–6 μm in length) were scored as properly oriented if the spindle spanned the bud neck and misoriented if the spindle resided entirely within the mother cell body. Wild type (WT), CUY1972 containing pCUB1263; *dyn1*Δ, CUY1930 containing pCUB1288; *nip100*Δ, CUY1991 containing pCUB1299. (B) Localization of dynein and dynactin proteins at microtubule plus ends and the SPB. Dynein and dynactin proteins were tagged with GFP and microtubules with mCherry-Tub1. Nip100-GFP, CUY2055 containing pCUB1293; Arp1-GFP, CUY2056 containing pCUB1293; Jnm1-GFP, CUY2057 containing pCUB1293; Dyn1-GFP, CUY2040 containing pCUB1299. White arrowheads indicate GFP signal on the ends of cytoplasmic microtubules; yellow arrowheads indicate cytoplasmic microtubule ends with no GFP signal. Scale bar, 2 μm. (C) Quantification of dynein and dynactin protein localization taken from images like those shown in B. (D) Coimmunoprecipitation of dynactin proteins. Cell lysates were incubated with anti-HA affinity gel. Precipitated material was run on SDS–PAGE and blotted for with either anti-HA (left) or anti-Myc (right) antibodies. Top row, Arp-HA Nip100-Myc (MY8960 containing pXX3; second row, Nip100-HA Ldb18-Myc (CUY1933 containing pXX3); third row, Jnm1-HA Arp1-Myc (CUY1936 containing pCUB1263); bottom row, Jnm1-HA Nip100-Myc (CUY1938 containing pCUB1263).

for *she1*Δ cells (Figure 3D). This indicates that even the weakened outer plaque connection provided by this fusion protein is still stronger than the normal half-bridge connection. Both of these results support the conclusion of the preceding section that the connection of cytoplasmic microtubules to the outer plaque is stronger than that at the half-bridge.

Overexpression of She1 inhibits dynactin complex localization to microtubule ends

Our observation that excessive cytoplasmic microtubule detachment in *she1*Δ cells depends on dynein activity is consistent with previous work suggesting that She1 negatively regulates dynein activity (Woodruff *et al.*, 2009). Thus we hypothesized that overexpression of She1 would produce a phenotype similar to that

caused by inhibiting dynein activity—specifically, the elongation of anaphase spindles within the mother cell. To test this, we imaged cells expressing She1 from the highly efficient *GAL1/10* promoter. We quantified the fraction of midanaphase spindles (between 3 and 6 μm) that were incorrectly oriented with both spindle poles in the mother cell. Cells overexpressing She1 had a level of spindle misorientation similar to that in *dyn1*Δ and *nip100*Δ cells (Figure 4A). Overexpressing She1 in *dyn1*Δ or *nip100*Δ cells did not increase their frequency of spindle misorientation, indicating that the She1 acts through the dynein pathway.

To investigate the mechanism of She1 inhibition of dynein activity, we overexpressed She1 in cells expressing GFP-tagged dynactin complex proteins and mCherry-Tub1 and scored cells for GFP signal at cytoplasmic microtubule plus ends and the SPB. For cells
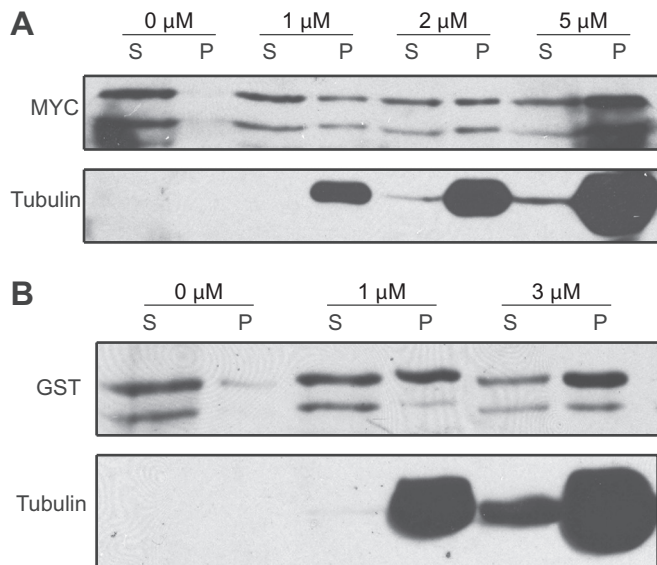
FIGURE 5: She1 associates with microtubules. (A) Lysate from cells expressing She1-13Myc (CUY1865) was incubated with various amounts of preassembled microtubules, the mixture centrifuged, and the supernatant (S) and pellet (P) fractions analyzed by Western blotting using anti-Myc (top) and anti-tubulin (bottom). Molar amounts of tubulin in microtubules used in each experiment are indicated above the lanes. (B) As in A, except that purified GST-She1 was used instead of cell lysates. Anti-GST antibody was used to visualize GST-She1.

expressing Nip100-GFP, Arp1-GFP, and Jnm1-GFP, She1 overexpression decreased the number of cells with plus-end labeling (nine-, seven-, and eightfold, respectively) and increased the number of cells with labeling only at the SPB (seven-, 17-, and fourfold, respectively; Figure 4, B and C). The overall number of cells that displayed a GFP signal was relatively unchanged. Overexpression of She1 did not substantially affect the localization of Dyn1-GFP (Figure 4, B and C).

One possible mechanism by which She1 could inhibit dynactin loading onto microtubule plus ends is by interfering with dynactin assembly. To test this possibility, we overexpressed She1-GFP and assessed the interaction between dynactin complex proteins by coimmunoprecipitation. Binding between Arp10-3HA and Nip100-13Myc, Nip100-3HA and Ldb18-13Myc, Jnm1-3HA and Arp1-13Myc, and Jnm1-3HA and Nip100-13Myc was not disrupted in cells overexpressing She1-GFP (Figure 4D). Thus, She1 does not appear to interfere with dynactin assembly. In addition, She1-GFP was not found in any of the immunoprecipitates, indicating that overexpression of She1-GFP does not disturb dynactin localization through direct interaction with its subunits (Supplemental Figure S1).

She1 associates directly with microtubules

As previously reported, She1-GFP localizes to mitotic spindles, cytoplasmic microtubules, and a ring structure at the bud neck (Wong et al., 2007; Woodruff et al., 2009). We assessed She1's ability to associate with microtubules by incubating whole-cell extracts of a strain expressing She1-13Myc with preassembled, Taxol-stabilized bovine microtubules. The microtubules were then spun down and the amount of She1-13Myc in the pellet and supernatant compared. She1-13Myc bound to microtubules in a microtubule concentration–dependent manner (Figure 5A). The apparent dissociation constant, equal to the concentration of polymerized tubulin required to cosediment half of the She1-13Myc, is ~2 μM. This association be-

tween She1 and microtubules could be direct or could be mediated by another protein in the cell extract. To determine whether She1 can bind directly to microtubules, we purified GST-She1 from bacterial cells and incubated it with Taxol-stabilized microtubules. GST-She1 bound to microtubules with an apparent dissociation constant of ~1 μM (Figure 5B). Thus She1 has the ability to bind to microtubules directly and with an affinity similar to that of other microtubule-associated proteins (Blake-Hodek et al., 2010).

DISCUSSION

We found that in cells lacking She1, cytoplasmic microtubules detach from the SPB at greatly elevated rates. This phenotype has also been noted by Markus et al. (2011). Microtubule detachment requires dynein activity; simultaneous loss of the dynactin protein Nip100 completely eliminates the she1Δ effect. This result agrees with previous reports indicating that She1 is a negative regulator of dynein function. This conclusion is also supported by our data showing that overexpression of She1 produces a defect in spindle orientation identical to that caused by loss of dynein or Nip100.

To determine how She1 inhibits dynein activity, we examined the localization of dynein and dynactin complex proteins in cells overexpressing She1. Whereas She1 overexpression has little effect on dynein localization, it greatly reduces the localization of dynactin proteins to cytoplasmic microtubule plus ends. This agrees with previous reports that loss of She1 allows dynactin components to localize to cytoplasmic microtubule plus ends at earlier points in the cell cycle (Woodruff et al., 2009) and in greater number (Markus et al., 2011). She1 overexpression does not affect the integrity of the dynactin complex, supporting the previous suggestion that She1 interferes with the interaction between dynein and dynactin (Woodruff et al., 2009; Markus et al., 2011). However, She1 did not coprecipitate with the dynactin complex, indicating that any interaction is transient. She1 was shown previously to associate with cytoplasmic microtubules during G1 and preanaphase, when dynein is inactive, but not during anaphase, when dynein is active (Woodruff et al., 2009). Our results show that She1 can bind directly to microtubules, leading to the possibility that She1 inhibits dynein activity by competing with dynactin for access to microtubules.

Although dynein activity is down-regulated during G1, it is still the major cause of microtubule detachment during this portion of the cell cycle; loss of Nip100 causes a fourfold decrease in microtubule detachment in G1 cells. On the other hand, Myo2, the type V myosin protein that is responsible for directing cytoplasmic microtubules to the bud in the early stages of the cell cycle and might therefore be expected to play a role in microtubule detachment in G1 cells, has relatively little effect on microtubule detachment. Even if we attribute all of the microtubule detachment in nip100Δ cells to Myo2 activity, it still amounts to only 25% of the rate in wild-type cells. In G1 cells lacking She1, which may contain maximal dynein activity, 95% of microtubule detachment can be attributed to dynein activity (as determined by comparing detachment in she1Δ vs. she1Δ nip100Δ cells). These results likely reflect the fact that dynein pulls harder on cytoplasmic microtubules than Myo2; in vitro studies show that cytoplasmic dynein generates more than twice the force of myosin V (Gennerich et al., 2007; Mehta et al., 1999).

Although dynein pulls on the SPB-distal plus ends of cytoplasmic microtubules, the breakage event occurs at the SPB. Detached microtubules always appear to be full length and most contain γ-tubulin and Spc72 at their minus ends. Because Spc72 binds Spc97 and Spc98 but not Tub4 (Knop and Schiebel, 1998), we assume that the entire γ-tubulin complex is present. Of interest, the γ-tubulin complex appears sufficient to stabilize the minus ends of detached

microtubules, because these microtubules disappear rapidly after loss of this structure. In G1-arrested cells, Spc72 is primarily unphosphorylated and binds to Kar1 in the half-bridge. A Spc72–Kar1 protein fusion greatly reduces microtubule detachment in G1 cells, indicating that the Spc72–Kar1 interaction is the weak link at the half-bridge. In metaphase cells, Spc72 is phosphorylated and binds to Nud1, which in turn binds Cnm67, in the outer plaque. However, fusing Spc72 to Cnm67 did not reduce microtubule detachment from the outer plaque. This could be taken as evidence that the Spc72 attachment is not the weak link in the outer plaque. On the other hand, one could simply argue that the Spc72–Cnm67 fusion damages the outer plaque sufficiently to allow microtubule detachment by an aberrant mechanism.

Microtubule detachment rates are higher in G1 cells than in M-phase cells. Three lines of evidence indicate that this difference is due to a weaker microtubule attachment to the SPB half-bridge, rather than a stronger pulling force, in G1 cells. 1) We used the kar1-Δ15 mutation to restrict microtubule nucleation to the outer plaque. This allowed us to measure the effect of she1Δ on microtubule detachment from both the half-bridge (she1Δ cells) and the outer plaque (kar1-Δ15 she1Δ cells) at the same point in the cell cycle (G1). The microtubule detachment rate from the half-bridge was fourfold higher than from the outer plaque. 2) We used the Spc72–Kar1 protein fusion to direct microtubule attachment to the half-bridge. This strengthens microtubule attachment to the half-bridge, but even this strengthened attachment is weaker than normal outer plaque attachment. Similarly, we used the Spc72-Cnm67 fusion protein to direct microtubule attachment to the outer plaque. This weakens microtubule attachment at the outer plaque, but even this weakened attachment is stronger than the normal half-bridge attachment. 3) If we assume that dynein is maximally active in she1Δ cells, then the pulling force should be equivalent in G1 and M phase she1Δ cells; however, microtubule detachment is eightfold more frequent in G1 cells. Thus we conclude that microtubule attachments to the outer plaque are stronger than those at the half-bridge.

It is not entirely clear why yeast nucleate cytoplasmic microtubules from two distinct locations on the SPB. Nucleation from both sites is not essential for vegetative growth; both the Spc72–Kar1 fusion, which confines nucleation to the half-bridge, and the Spc72–Cnm67 fusion, which confines nucleation to the outer plaque, allow cells to grow (Pereira et al., 1999; Gruneberg et al., 2000). However, microtubules coming from the half-bridge are essential for karyogamy (Conde and Fink, 1976; Pereira et al., 1999) and, because mating occurs only between cells arrested in G1 by mating factors, it follows that the half-bridge would be the predominant site of microtubule nucleation in cycling G1 cells. The switch to the outer plaque as cells enter mitosis may be made in part to withstand the pulling forces exerted by dynein, which is most active in the later portions of the cell cycle.

MATERIALS AND METHODS
Yeast strains and plasmids
Yeast strains used in this study are S288C or derivatives and are listed in Supplemental Table S2. Plasmids used are listed in Supplemental Table S3.

MATa cells were arrested in G1 by adding 3 μg/ml α-factor to the medium for 3 h. Cells containing P_{MET3}-CDC20-3HA were arrested in metaphase by adding 20 μg/ml methionine to the medium for 3 h. She1 was overexpressed in cells containing $P_{GAL1/10}$-SHE1, $P_{GAL1/10}$-SHE1-GFP, or $P_{GAL1/10}$-SHE1-13MYC by growing cultures to log phase in 2% raffinose medium for several generations and then shifting them to 2% galactose medium for 4–6 h.

Microscopy and image analysis
Images were obtained using a spinning disk confocal system as previously described (Huang and Huffaker, 2006). All images are maximum-intensity projections of z-series stacks (Δz = 0.7 μm). Analysis was performed using ImageJ (National Institutes of Health, Bethesda, MD). The mean values and standard deviations of microtubule detachment were determined using the Poisson approximation to the binomial distribution.

Microtubule cosedimentation assays
For assays using whole-cell extracts, log-phase yeast cells expressing She1-13Myc (CUY1865) were centrifuged for 5 min at 2000 rpm, washed with lysis buffer (80 mM 1,4-piperazinediethanesulfonic acid [PIPES], 1 mM ethylene glycol tetraacetic acid [EGTA], 1 mM MgSO4, 5% glycerol, 100 mM KCl, 0.25% Brij-35, 2 mM dithiothreitol [DTT], pH 6.8), and resuspended in lysis buffer containing 20 μM Taxol, 1 mM phenylmethylsulfonyl fluoride, 10 μg/ml leupeptin, and 10 μg/ml pepstatin. Cells were lysed in a bead beater, and lysates were precleared by centrifugation at 350,000 × g for 5 min at 4°C. Tubulin (Cytoskeleton, Denver, CO) was diluted to 1 mg/ml in PEM-DGT (100 mM PIPES, 2 mM EGTA, 1 mM MgCl2, 20 μM Taxol, 1 mM GTP, and 4 mM DTT) and precleared by centrifugation at 150,000 × g for 5 min at 4°C. The supernatant was incubated at 37°C for 20 min to allow microtubule polymerization, followed by centrifugation at 35,000 × g for 20 min at room temperature. The microtubule pellet was resuspended in PEM-DGT to a final concentration of 5 mg/ml. Various amounts of microtubules were added to 20 μl of precleared yeast cell lysate and incubated for 20 min on ice. Samples were centrifuged at 175,000 × g for 10 min at 4°C. Supernatant and pellet fractions were analyzed by SDS–PAGE and Western blotting using 9E10 anti-Myc (Covance, Princeton, NJ) and DM1α anti-tubulin (Sigma-Aldrich, St. Louis, MO) antibodies.

For assays using purified protein, She1–glutathione S-transferase (GST) was expressed in BL21 Escherichia coli cells containing plasmid pXX6. Cells were grown at 26°C in 1 l of Luria–Bertani broth containing 50 μg/ml kanamycin and then induced by adding 50 μM isopropyl-β-D-thiogalactoside for 4 h. Cells were then spun down, washed with cold phosphate-buffered saline (PBS), and resuspended in 8.5 ml of cold PBS containing EDTA-free protease inhibitors (Roche, Basel, Switzerland). Cells were lysed by the addition of 10 μl of 100 mg/ml lysozyme for 30 min, followed by sonication. Triton X-100 was added to 1% and the mixture rocked at 4°C for 20 min. Cell debris was pelleted at 12,000 × g for 25 min at 4°C. The supernatant was incubated with glutathione–Sepharose beads for 2.5 h at 4°C. Beads were then pelleted, washed four times with cold PBS, resuspended in 350 μl of 80 mM reduced glutathione in PBS (pH 7), and rocked for 16 h at 4°C. Purified GST-She1 was then obtained by adding the mixture to a minichromatography column (Bio-Rad, Hercules, CA) and spinning at 5000 × g for 2 min. GST-She1 was incubated with assembled microtubules at room temperature for 5 min and then spun at 175,000 × g for 40 min. Supernatant and pellet fractions were analyzed by SDS–PAGE and Western blotting using anti-GST antibodies.

Coimmunoprecipitations
Coimmunoprecipitations were performed as described previously (Wolyniak et al., 2006), except that anti-hemagglutinin (HA) affinity gel or anti-Myc affinity gel (Sigma-Aldrich) was used to precipitate epitope-tagged proteins from cell lysates. Western blots were probed with either 9E10 anti-Myc or HA.11 anti-HA antibodies (Covance).

REFERENCES

Blake-Hodek KA, Cassimeris L, Huffaker TC (2010). Regulation of microtubule dynamics by Bim1 and Bik1, the budding yeast members of the EB1 and CLIP-170 families of plus-end tracking proteins. Mol Biol Cell 21, 2013–2023.

Byers B, Goetsch L (1975). Behavior of spindles and spindle plaques in the cell cycle and conjugation of *Saccharomyces cerevisiae*. J Bacteriol 124, 511–523.

Conde J, Fink GR (1976). A mutant of *Saccharomyces cerevisiae* defective for nuclear fusion. Proc Natl Acad Sci USA 73, 3651–3655.

Desai A, Mitchison TJ (1997). Microtubule polymerization dynamics. Annu Rev Cell Dev Biol 13, 83–117.

Farkasovsky M, Küntzel H (1995). Yeast Num1p associates with the mother cell cortex during S/G2 phase and affects microtubular functions. J Cell Biol 131, 1003–1014.

Gennerich A, Carter AP, Reck-Peterson SL, Vale RD (2007). Force-induced bidirectional stepping of cytoplasmic dynein. Cell 131, 952–965.

Gruneberg U, Campbell K, Simpson C, Grindlay J, Schiebel E (2000). Nud1p links astral microtubule organization and the control of exit from mitosis. EMBO J 19, 6475–6488.

Heil-Chapdelaine RA, Oberle JR, Cooper JA (2000). The cortical protein Num1p is essential for dynein-dependent interactions of microtubules with the cortex. J Cell Biol 151, 1337–1344.

Hoepfner D, Brachat A, Philippsen P (2000). Time-lapse video microscopy analysis reveals astral microtubule detachment in the yeast spindle pole mutant cnm67. Mol Biol Cell 11, 1197–1211.

Huang B, Huffaker TC (2006). Dynamic microtubules are essential for efficient chromosome capture and biorientation in *S. cerevisiae*. J Cell Biol 175, 17–23.

Hwang E, Kusch J, Barral Y, Huffaker TC (2003). Spindle orientation in *Saccharomyces cerevisiae* depends on the transport of microtubule ends along polarized actin cables. J Cell Biol 161, 483-488.

Jaspersen SL, Winey M (2004). The budding yeast spindle pole body: structure, duplication, and function. Annu Rev Cell Dev Biol 20, 1–28.

Knop M, Schiebel E (1997). Spc98p and Spc97p of the yeast gamma-tubulin complex mediate binding to the spindle pole body via their interaction with Spc110p. EMBO J 16, 6985–6995.

Knop M, Schiebel E (1998). Receptors determine the cellular localization of a gamma-tubulin complex and thereby the site of microtubule formation. EMBO J 17, 3952–3967.

Korinek WS, Copeland MJ, Chaudhuri A, Chant J (2000). Molecular linkage underlying microtubule orientation toward cortical sites in yeast. Science 287, 2257–2259.

Lee L, Tirnauer JS, Li J, Schuyler SC, Liu JY, Pellman D (2000). Positioning of the mitotic spindle by a cortical-microtubule capture mechanism. Science 287, 2260–2262.

Lee WL, Kaiser M, Cooper JA (2005). The offloading model for dynein function: differential function of motor subunits. J Cell Biol 168, 201–207.

Markus SM, Lee WL (2011). Regulated offloading of cytoplasmic dynein from microtubule plus ends to the cortex. Dev Cell 20, 639–651.

Markus SM, Plevock KM, St Germain BJ, Punch JJ, Meaden CW, Lee WL (2011). Quantitative analysis of Pac1/LIS1-mediated dynein targeting: implications for regulation of dynein activity in budding yeast. Cytoskeleton 68, 157–174.

Marschall LG, Jeng RL, Mulholland J, Stearns T (1996). Analysis of Tub4p, a yeast gamma-tubulin-like protein: implications for microtubule-organizing center function. J Cell Biol 134, 443–454.

Mehta AD, Rock RS, Rief M, Spudich JA, Mooseker MS, Cheney RE (1999). Myosin-V is a processive actin-based motor. Nature 400, 590–593.

Moore JK, Stuchell-Brereton MD, Cooper JA (2009). Function of dynein in budding yeast: mitotic spindle positioning in a polarized cell. Cell Motil Cytoskeleton 66, 546–555.

O'Toole ET, Winey M, McIntosh JR (1999). High-voltage electron tomography of spindle pole bodies and early mitotic spindles in the yeast *Saccharomyces cerevisiae*. Mol Biol Cell 10, 2017–2031.

Pereira G, Grueneberg U, Knop M, Schiebel E (1999). Interaction of the yeast gamma-tubulin complex-binding protein Spc72p with Kar1p is essential for microtubule function during karyogamy. EMBO J 18, 4180–4195.

Spang A, Geissler S, Grein K, Schiebel E (1996). gamma-Tubulin-like Tub4p of *Saccharomyces cerevisiae* is associated with the spindle pole body substructures that organize microtubules and is required for mitotic spindle formation. J Cell Biol 134, 429–441.

Usui T, Maekawa H, Pereira G, Schiebel E (2003). The XMAP215 homologue Stu2 at yeast spindle pole bodies regulates microtubule dynamics and anchorage. EMBO J 22, 4779–4793.

Vallen EA, Hiller MA, Scherson TY, Rose MD (1992). Separate domains of KAR1 mediate distinct functions in mitosis and nuclear fusion. J Cell Biol 117, 1277–1287.

Wolyniak MJ, Blake-Hodek K, Kosco K, Hwang E, You L, Huffaker TC (2006). The regulation of microtubule dynamics in *Saccharomyces cerevisiae* by three interacting plus-end tracking proteins. Mol Biol Cell 17, 2789–2798.

Wong J *et al.* (2007). A protein interaction map of the mitotic spindle. Mol Biol Cell 18, 3800–3809.

Woodruff JB, Drubin DG, Barnes G (2009). Dynein-driven mitotic spindle positioning restricted to anaphase by She1p inhibition of dynactin recruitment. Mol Biol Cell 20, 3003–3011.

Yin H, Pruyne D, Huffaker TC, Bretscher A (2000). Myosin V orientates the mitotic spindle in yeast. Nature 406, 1013–1015.